

**Research  
Article**

# *Extreme Loads for an Offshore Wind Turbine using Statistical Extrapolation from Limited Field Data*

**Puneet Agarwal and Lance Manuel\***, Department of Civil, Architectural, and Environmental Engineering, University of Texas, Austin, TX 78712, USA

**Key words:**

Offshore wind turbines;  
statistical load extrapolation;  
extreme loads;  
bootstrap techniques

*When interest is in establishing extreme loads for wind turbines, it is common to either carry out extensive simulation studies or undertake a field measurement campaign. At the Blyth offshore wind farm in the UK, a 2 MW wind turbine was instrumented, and environment and load data were obtained in a previous study. Here, we discuss how such data, even though very limited, may be used along with parametric models to establish extreme loads associated with return periods on the order of 20–50 years. The environmental characteristics at the Blyth site are such that wind and waves are of primary importance. Distributions for the extreme mudline bending moment are established using parametric models. Long-term loads are derived for different wind regimes possible at the site and the results are compared. Using bootstrap techniques, the effect of variability in the parameters for load distribution is investigated. Copyright © 2008 John Wiley & Sons, Ltd.*

*Received 22 November 2006; Revised 17 September 2008; Accepted 21 September 2008*

## **Introduction**

Our objective here is to estimate extreme loads for an offshore wind turbine for which the environmental and load data are available from field measurements. Using a probabilistic approach, we will estimate long-term loads associated with a target failure probability, or equivalently, a prescribed service life for the turbine. In the probabilistic approach, variables describing the wind and wave environment as well as the turbine response are modelled as random variables whose probabilistic distributions need to be established. In general, the required data may be obtained either from simulations with a turbine model or from the field measurements on the turbine. While data obtained from the simulations can ensure the inclusion of a wide range of environmental input variables and resulting response statistics, simulation models are limited by how closely they can represent the wind turbine. Data obtained from full-scale field measurements, on the other hand, provide a true representation of the turbine response subjected to observed environmental conditions. Field data, however, can be ‘limited’ in the sense that, when available, they are generally recorded only for a finite duration of time, and may not cover all possible environmental conditions expected to occur over the life of the turbine. Therefore, when using limited field data, statistical parametric or non-parametric techniques are often used to

\*Correspondence to: L. Manuel, Department of Civil, Architectural, and Environmental Engineering, University of Texas at Austin, 1 University Station C1748, Austin, TX 78712, USA.  
E-mail: lmanuel@mail.utexas.edu

extrapolate the loads from observed events to loads associated with prescribed safety levels. Statistical extrapolation techniques have been used to predict both long-term extreme and fatigue loads for wind turbines. Examples of such studies include those by Moriarty *et al.*<sup>9</sup> and Fitzwater and Winterstein<sup>8</sup>. It is worth noting that field data available from campaigns, such as the one reported on here, may be used to validate simulation models that form the basis for design load computations. In the present case, neither the simulation studies for the test turbine nor the simulation models were available; hence, no validation studies could be carried out.

In the present study, we use statistical load extrapolation procedures to estimate long-term loads using limited field data recorded at an offshore wind turbine. We focus our attention on the bending moment at the mudline as the load variable of interest. The turbine under consideration is an instrumented 2 MW wind turbine at the Blyth wind farm, which is located about 1 km off the northeast coast of England, and for which data were recorded for about 16 months. Key features of the site pertinent to the present study include contrasting characteristics of the environment and response characteristics associated with winds blowing from the shore to the sea versus those associated with winds blowing from the sea to the shore. In addition, the turbine located in shallow water is likely subjected to breaking waves. We will discuss the possible importance of these features in estimation of long-term loads using the statistical extrapolation procedure.

### Statistical Load Extrapolation

In reliability-based design of wind turbines, one is required to estimate extreme loads associated with a prescribed level of safety, e.g. a required service life. The appropriate long-term load,  $l_T$ , corresponding to a service life of  $T$  years ( $T$  would ordinarily be on the order of 20 years for an offshore wind turbine) needs to be determined by consideration of the probabilistic distribution for all important environmental random variables, as well as for the turbine load conditional on the environment. We assume here that the environment for the turbine under consideration is defined by the 10 min mean wind speed at the turbine nacelle, denoted by the random variable  $V$ , and the significant wave height, denoted by  $H_s$ . The variables  $H_s$  and  $V$  are modelled as jointly distributed random variables. The turbine load of interest,  $L$ , depends on  $V$  and  $H_s$ , and is thus an implicit function of the environmental random variables. For the target failure probability,  $P_T$ , associated with the service life,  $T$ , we are interested in estimating  $l_T$  such that:

$$P_T = P[L > l_T] = \iint_{H_s, V} P[L > l_T | (V, H_s)] f_{V, H_s}(v, h) dv dh \quad (1)$$

where  $f_{V, H_s}(v, h)$  is the joint probability density function of the environmental random variables. Equation (1) makes it possible to estimate the long-term probability of exceedance of any specified load by integrating short-term load distributions conditional on  $V$  and  $H_s$ , with the relative likelihood of all  $(V, H_s)$  pairs. As such, the form of equation (1) enables one to directly compute the probability of exceedance, or the failure probability for a given load level. Our purpose, however, is to estimate the long-term load associated with a given exceedance probability. To this end, we will construct the probability of load exceedance curve for various assumed load levels; then, using this exceedance probability curve that represents the long-term distribution of loads, we can simply read off the long-term load associated with the prescribed level of safety or the target exceedance probability.

In order to be able to use equation (1), one needs to establish the joint distribution for wind speed and wave height as well as the conditional distribution of the load given  $V$  and  $H_s$ . We will use parametric probability distributions to describe all the random variables. To estimate the parameters of these distributions, we will use the field data recorded at the Blyth site. Since the field data are limited, the parametric distributions may not accurately represent true conditions at the site. We will address details regarding statistical uncertainty in long-term load estimation because of limited field data by making use of bootstrap techniques.<sup>1</sup> Next, we briefly discuss the Blyth site and the recorded data, and then present the distributions of the random variables of interest in this study.

## **Blyth Site**

The Blyth project is an experimental wind farm consisting of two 2 MW Vestas V66 wind turbines. The Blyth site is located on the north-east coast of England, off the Northumberland shore. The wind turbines are located approximately 1 km from the shoreline. The mean water depth at the instrumented turbine varies between a Lowest Astronomical Tide (LAT) level of 6 m and a Mean High Water Springs level of 11 m. The average water depth at the turbine location is approximately 9 m. One of the two turbines at Blyth was instrumented as part of a research project funded by the European Commission; it has a hub height of 62 m above the LAT level and a blade diameter of 66 m. The turbines are located on a sharply sloping submerged rock, known as the 'North Spit', in rock–socket type foundations. This local bathymetry results in rather large breaking waves at the turbine.

Field measurements were collected for 16 months between October 2001 and January 2003, thus covering more than one full winter season. While almost 64 000 data sets or 10 min samples were continuously recorded, only about 2300 data sets (equivalent to only about 16 days) were found to be usable after bad or missing data were discarded. Measured data included wind speed and direction at the nacelle, sea surface elevation and bending moments at several vertical stations along the tower and the pile. One of these stations—the mudline bending moment—is our load variable of interest here. The nacelle wind speed data were calibrated such that the mean wind speed measured at the nacelle was approximately equal to the mean free wind speed measured at a similar elevation at a nearby shore location. The wave climate data were measured using a wave radar system located at the entrance platform of the turbine, 11.7 m above the LAT line. Additional details regarding the data and measurement system may be found in Camp *et al.*<sup>2</sup>

Time series data in 10 min segments were sampled at 40 Hz, and the minimum, maximum, mean and standard deviation for each channel were recorded as part of the statistics comprising the 'summary' data sets. From these summary data sets, we focus our attention on the mean wind speed,  $V$ , at the nacelle, and the significant wave height,  $H_s$ , obtained from the sea surface elevation, as the environment variables of interest. For the load variable, we consider the absolute maximum (the larger of the maximum positive and negative values) of the mudline bending moment,  $M$ , in one of two available orthogonal components.

## **Description of Environment And Response**

Of central importance in the evaluation of the exceedance probability, using equation (1), is the estimation of distributions of the random variables defining the environment and the response conditional on the environment. We discuss next our procedure for deriving these distributions from the available field data at the Blyth site.

### **Environment Random Variables**

We assume that the environment at the Blyth site is adequately described by the mean wind speed,  $V$ , and the significant wave height,  $H_s$ . Both of these variables are based on 10 min statistics. Before we present the distributions for these variables, we believe it is instructive to study the wind and wave data that we use to establish the respective distributions. A scatter diagram of the mean wind speed and significant wave height data is shown in Figure 1(a). It is useful to study separately the data associated with 'onshore' and 'offshore' wind directions. Here, onshore winds will refer to winds that blow towards the shore from the sea, while offshore winds will refer to winds that blow towards the sea from the shore. Thus, all 10 min data for which the mean direction is between  $0^\circ$  and  $140^\circ$  are treated as onshore winds, while data for which the mean wind direction is between  $180^\circ$  and  $325^\circ$  are treated as offshore winds<sup>2</sup>. A third control set, consisting of all of the available data, regardless of associated wind direction, is treated as the 'all-direction' winds in this study. It may be seen from Figure 1a that there is significant scatter in the data, with onshore and offshore winds following markedly different trends. The onshore winds suggest greater correlation between wind speed and wave heights, which is possibly because of the longer fetch associated with onshore winds. Another feature of inter-

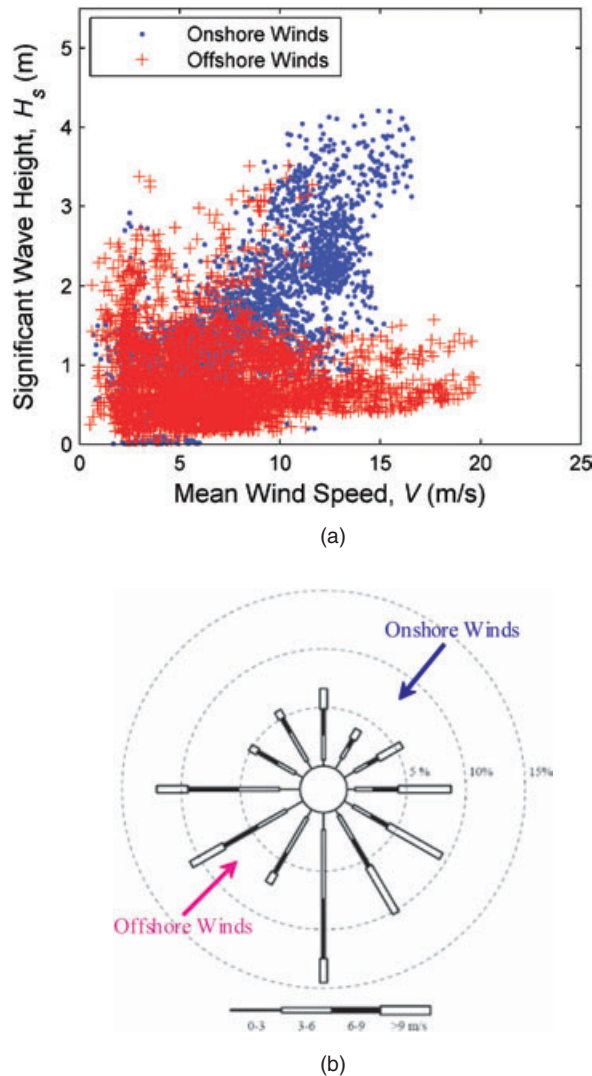


Figure 1. (a) Wind-wave scatter diagram and (b) wind rose<sup>2</sup>

est is the presence of some fairly high wave heights associated with relatively low wind speeds, a feature more prominent in the offshore wind data since this would not be expected in open seas where larger wave heights are generally associated with higher wind speeds. The distribution of wind speeds and directions, as presented in the wind rose in Figure 1b, suggests that onshore winds are associated with a greater relative frequency of higher wind speeds than lower wind speeds. This is in contrast with the offshore wind data where lower wind speeds are more common. This is reflected in the respective mean wind speeds for each data set separately. The mean wind speeds are 9.57, 6.25 and 7.70  $\text{m s}^{-1}$ , respectively, for the onshore, offshore and all-direction winds.

We assume that the mean wind speed,  $V$ , follows a Rayleigh distribution, as is done, for example, in the International Electrotechnical Commission (IEC) design guidelines.<sup>3,4</sup> We are interested here in studying loads that arise while the turbine is operating. Accordingly, the Rayleigh distribution is truncated both below a cut-in wind speed,  $V_{in}$ , of 4  $\text{m s}^{-1}$ , and above a cut-out wind speed,  $V_{out}$ , of 25  $\text{m s}^{-1}$ . The expression for the truncated cumulative distribution function (CDF),  $F_V(v)$ , of  $V$  is thus:

$$F_V(v) = \frac{G(V_{in}) - G(v)}{G(V_{in}) - G(V_{out})}; \quad G(v) = \exp\left[-\left(\frac{v}{\alpha}\right)^2\right] \tag{2}$$

where  $\alpha$  is a single parameter of the Rayleigh distribution that can be estimated from the average value of  $V$ .

To represent the variability in the wave climate and account for the dependence of wave heights on wind speed, we assume that the random variable,  $H_s$ , the significant wave height, conditional on the mean wind speed,  $V$ , follows a Weibull distribution (as is done, for example, in the offshore standard, Det Norske Veritas (DNV)-OS-J101.<sup>5</sup> The expression for the CDF of  $H_s$  conditional on  $V$ , namely  $F_{H_s|V}(h)$ , is given by:

$$F_{H_s|V}(h) = 1 - \exp\left[-\left(\frac{h}{\eta(v)}\right)^{k(v)}\right] \tag{3}$$

Both the shape parameter,  $k$ , and the scale parameter,  $\eta$ , of the Weibull distribution depend on the mean wind speed. They are estimated on the basis of the available summary data, and quadratic polynomials in mean wind speed were found to yield good estimates for  $k$  and  $\eta$  as functions of the mean wind speed.

### Turbine Load

For the turbine load (or response) random variable, we focus our attention on the absolute 10 min maximum (larger of the maximum positive and negative values) of the mudline bending moment in one of two available orthogonal components, fixed in space. Hereinafter, we refer to this load variable simply as the mudline bending moment and denote it by  $M$ . We choose to represent the random variable,  $M$ , by a two-parameter Gumbel distribution, conditional on the environmental variables,  $V$  and  $H_s$ . The cumulative distribution function for  $M$  is given by:

$$F_{M|V,H_s}(m) = \exp\left[-\exp\left[-\left(\frac{m - u(v, h)}{\beta(v, h)}\right)\right]\right] \tag{4}$$

The Gumbel parameters,  $u$  (modal value) and  $\beta$  (measure of dispersion), are dependent on  $V$  and  $H_s$ , and are evaluated from the available ( $V, H_s, M$ ) data. To this end, the data are binned into ( $V, H_s$ ) cells and the parameters,  $u$  and  $\beta$ , are estimated for each cell. A cell size of 2 m s<sup>-1</sup> in the  $V$  direction and 0.5 m in the  $H_s$  direction is used. The parameters  $u$  and  $\beta$  are estimated using the method of moments, with distribution fits adjusted sometimes in order to obtain a better representation of tail fits because of our interest in extreme loads that require extrapolation to higher load levels than were recorded.

The parameters,  $u$  and  $\beta$ , thus obtained, are presented in Figure 2, for the all-direction winds only. It is observed from Figure 2 that both parameters exhibit very high variability with respect to the environmental variables. This precludes development of a smooth surface fit over all the values of  $V$  and  $H_s$  of interest, which would have yielded a simple closed-form conditional distribution of the random variable  $M$  (given  $V$  and  $H_s$ ). Figure 2 also highlights the limitations of using recorded data, which was alluded to earlier. It is observed that data are not available for many cells (shown by zero values of the parameters)—most notably at large ( $V, H_s$ ) values. We estimate Gumbel parameters for these ‘empty’ cells by using a weighted average of all non-empty cells based on inverse-squared distance (in  $V$ - $H_s$  space). The Gumbel parameters for the offshore and onshore wind cases not shown in Figure 2 are based on data that are subsets of the all-direction wind data, and they follow similar non-smooth trends with  $V$  and  $H_s$ .

The highly variable behaviour of the load distribution parameters with respect to the environmental variables, as discussed, is mainly due to the scarcity of data in most bins. For example, out of the 50 ( $V, H_s$ ) bins that have any data at all for the all-direction winds, 30 bins have fewer than 40 data, and 21 bins have fewer than 20 bins. The available data are even scarcer when divided into onshore and offshore winds. Such scarcity of data precludes binning using more than two environmental variables. If additional data were available,

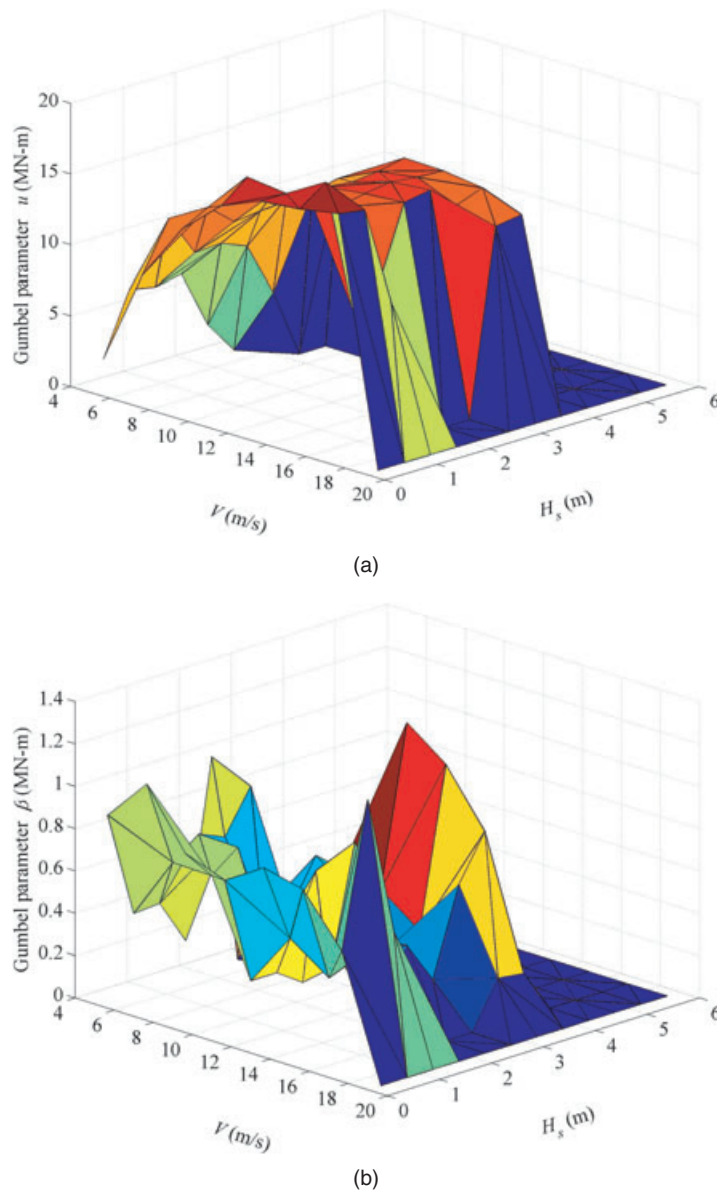


Figure 2. Variation of Gumbel parameters, (a)  $u$  and (b)  $\beta$ , with mean wind speed  $V$ , and significant wave height  $H_s$ , for all-direction winds. Estimates at the centres of the  $(V, H_s)$  cells are shown

turbulence intensity (or turbulence standard deviation,  $\sigma_V$ ), which might be expected to influence turbine loads to some degree, might have been considered as a third environmental random variable, in addition to  $V$  and  $H_s$ . On this latter point, in a related article,<sup>6</sup> the authors considered the use of two alternative random variables,  $(V, \sigma_V)$ , instead of  $(V, H_s)$  considered here [while the use of three environmental random variables makes it difficult to obtain a sufficient number of data in each 3-D bin, the 2-D  $(V, \sigma_V)$  binning is more reasonable to apply]. For the same data sets used here, it was found that even though there is some influence on long-term loads by including  $\sigma_V$  as a random variable, this effect is only of secondary importance to  $V$  and is comparable with the importance of  $H_s$ .



### Application and Results

Once the distributions for the environmental and load random variables are obtained, we can establish the probabilistic distribution of long-term loads, and thus estimate long-term loads using equation (1). The integrand in equation (1) cannot be evaluated analytically; however, since not all the involved distribution functions there are available in closed form. Accordingly, we evaluate the integral using a finite summation that again involves dividing the  $V$ - $H_s$  plane into cells of equal size. The contribution to the probability of exceedance of a given load level from each cell is computed by evaluating the load distribution at the centre of the cell, under the assumption that the distribution remains fairly constant over each cell. The total probability is finally obtained by summing contributions from all the cells, as expressed by the following double summation:

$$P_T \approx \sum_{i=1}^{N_V} \sum_{j=1}^{N_H} [1 - F_{L|V,H_s}(l_T)|v_i, h_j] f_{V,H_s}(v_i, h_j) \Delta V \Delta H_s \tag{5}$$

where  $N_V$  and  $N_H$  denote the number of cells along the  $V$  and  $H_s$  directions, respectively. The width of the cells is denoted by  $\Delta V$  and  $\Delta H_s$  in each of the directions. Each cell  $(i, j)$  has central value  $(v_i, h_j)$ . We use the same cell widths as were used to estimate the turbine load distribution parameters—namely,  $2 \text{ m s}^{-1}$  in the  $V$  direction and  $0.5 \text{ m}$  in the  $H_s$  direction. This leads to a total of 96 cells when we evaluate the summation for wind speeds between  $4$  and  $20 \text{ m s}^{-1}$ , and for significant wave heights up to  $6 \text{ m}$ . The upper bounds for  $V$  and  $H_s$  were verified to be satisfactory for the purposes of these computations, primarily due to the low probability associated with higher wind speed and significant wave height levels.

The long-term load exceedance probability (i.e. the probability of exceeding specified levels of  $M$  in 10 min), computed using equation (5), is shown in Figure 3 with the thicker lines, for all three wind direction cases—namely, the all-direction, onshore and offshore winds. It is observed that at higher load levels associated with longer return periods, the exceedance probability in offshore winds is generally higher than for all-direction winds, while this probability for onshore winds is significantly lower (by two to three orders of magnitude). The exceedance probability curve for the all-direction winds lies between the probability curves for the onshore and offshore winds as might be expected, since the all-direction winds include the onshore and offshore winds as subsets. The long-term load for a specified target probability (or return period) may be estimated from the

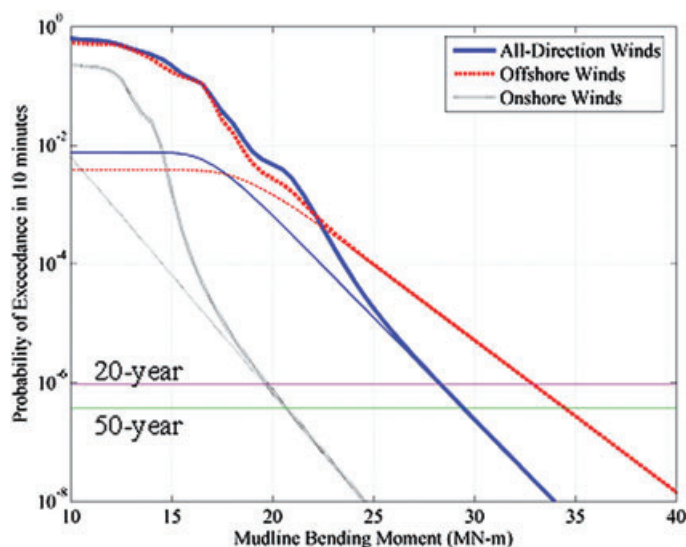


Figure 3. Probability of load exceedance curves for the three wind direction cases. The thick lines represent the total probability, while the thin lines represent contributions only from significant cells identified in Figure 4

Table I. Long-term loads for different wind directions

Return period (years)	Long-term load (MN-m)		
	All-direction	Offshore	Onshore
20	28.3	32.9	19.7
50	29.4	34.4	20.7

exceedance probability curves in Figure 3. Results for 20 and 50 year return periods are summarized in Table 1—for example, the long-term load for a 20 year return period is found to be 28.3, 32.9 and 19.7 MN-m, respectively, for the all-direction, offshore and onshore winds. Small increases in these loads are seen at the higher 50 year return period level.

We now study the relative contribution of different ( $V, H_s$ ) cells to the total probability of exceedance of a given load level. This enables one to determine the most significant environmental conditions that govern the overall risk. Figure 4 shows the fractional contribution of each cell to the exceedance probability associated with a 20 year return period load. It is observed that, for all three wind direction cases, a single cell alone makes almost the entire contribution to the overall exceedance probability; we refer to these cells as significant cells in the following. The exceedance probability curves for these significant cells are plotted in Fig 3 using thin lines. It may be seen that these cells contribute almost all of the probability at high loads, which include the long-term loads presented earlier for the 20 and 50 year return periods. To understand why only a few individual cells identified in Figure 4 contribute significantly to the total exceedance probability, we note that the long-term load exceedance probability is obtained by summing, from each cell, the product of the short-term distribution of loads (given the environment) and the environment distribution itself, as described by equation (5). In this study, it is found that for all three cases, contributions from the significant cells are large due mainly to the large short-term load exceedance conditional probability. This, in turn, is because of large estimates of Gumbel parameters,  $u$  and  $\beta$ , for the significant cells compared with those for other cells in the three wind direction cases. It should be pointed out that the results presented and the conclusions regarding significant cells are directly dependent on the available data, which are extremely limited in some cells.

Because estimates of the parameters for the distributions of the load variable,  $M$ , greatly influence the results, it is important to investigate the effect of variability or uncertainty in these parameters on predicted long-term loads. This variability stems from the relative scarcity of data in some cells as well as from the uncertainty associated with statistical estimation of the parameters using the data that are available. We discuss the effect of variability in parameters in the following.

### *Variability in Parameters for Load Distribution*

We study the effect of uncertainty in the parameters,  $u$  and  $\beta$ , for the short-term load distribution,  $M$ , conditional on environmental variables,  $V$  and  $H_s$ , and the resulting variability in the predicted long-term loads. In order to quantify this variability, we use non-parametric bootstrap techniques<sup>1</sup> that rely on randomly resampling data, say  $N_r$  times, and then estimating parameters,  $u$  and  $\beta$ , for each resampling, using the same approach followed for the mean (no-variability) parameter predictions that were presented before (in Figure 2). Using the set of  $N_r$  estimates for the two parameters, it is possible to obtain appropriate statistics such as the mean value and standard deviation of each parameter, which helps to quantify the variability in that parameter. We study the effect of variability in these parameters on the long-term load exceedance distribution by computing exceedance probability curves for each of the resamplings, and then computing 5- and 95-percentile levels of probability for a specified load level. These can then be used to provide confidence bounds on our mean value (no variability) estimates of long-term loads for specified return periods.

The effect of the variability in parameters of the short-term load distribution is presented in Figure 5, which shows the 5- and 95-percentile values of the exceedance probability, for a given load level. The curves shown



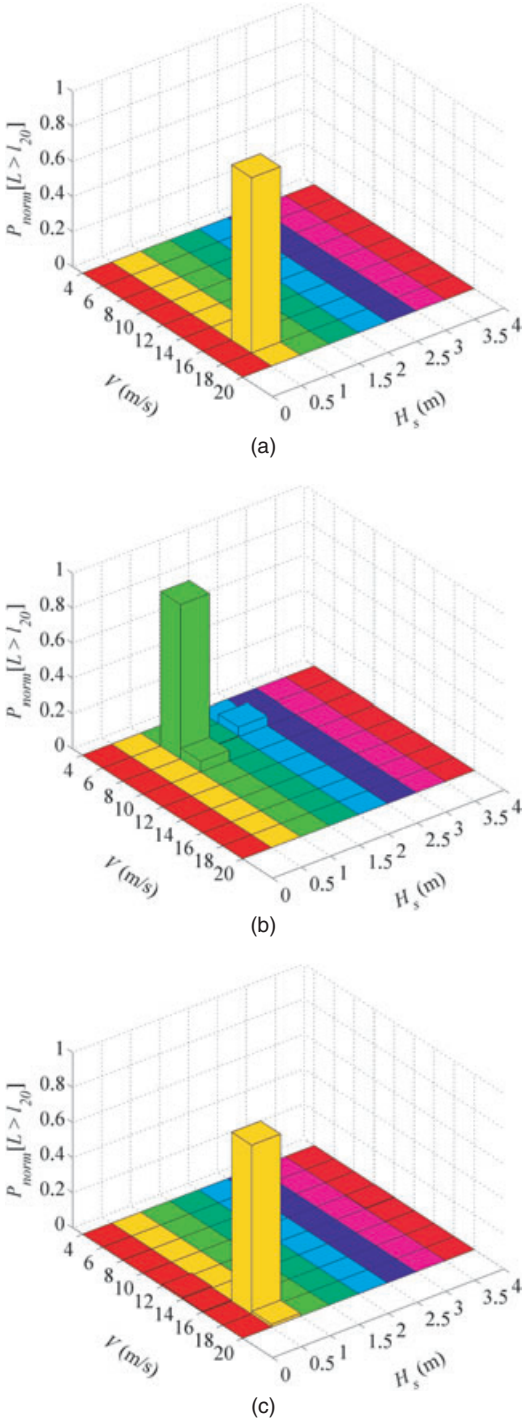


Figure 4. Fractional contributions of individual ( $V, H_s$ ) cells to the normalized probability,  $P_{norm}$ , representing the cell probability divided by the total probability of exceeding the 20 year design load for (a) offshore winds, (b) onshore winds and (c) all-direction winds. Significant cells are the cells with the largest contributions

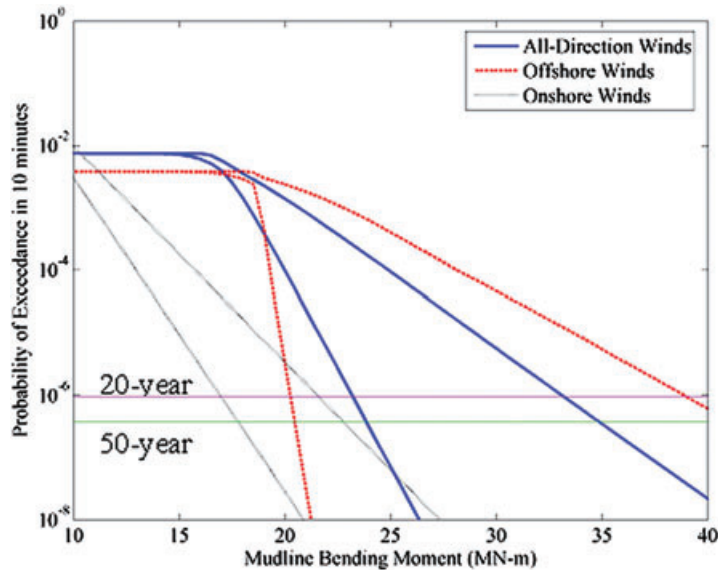


Figure 5. Probability of load exceedance curves at the 5- and 95%-confidence levels based on bootstrapping of recorded loads data. Results shown are for significant cells only

are only for the significant cells (i.e. the cells contributing most to total probability, as indicated in Figure 4). It is evident from these curves that, for any given planned service life or return period, the range of predicted long-term loads can be very large, which is a direct result of the limited data available. For example, for the all-direction winds, the 5- and 95-percentile long-term loads for a 20 year service life are about 23 and 33 MN-m, respectively. This range represents greater than 30% of the mean load prediction (see Table 1). The effect of variability is most prominent for offshore winds and least so for onshore winds. Onshore wind loads exhibit the lowest uncertainty because the significant cell for this case had a larger amount of data (58 records) than was the case for the offshore and all-direction winds. Moreover, the Gumbel parameters estimated in this case led to a very good distribution fit to the data; hence, bootstrap resamplings did not introduce large variability in the parameter values and thus in the long-term loads. The significant cell in the offshore winds, on the other hand, had much less data (only 32 records) and these data exhibited relatively large scatter, leading to worse fits from parameter uncertainty out of the bootstrap resamplings. This, in turn, led to significant uncertainty in long-term load predictions for the offshore case. The variability in long-term loads for the all-direction case was not as large as in the onshore case but not as small as in the offshore case.

### Discussion

In order to interpret the various results presented from a physical point of view, a question of particular interest relates to why the long-term loads are governed by offshore winds, even though the mean wind speed for the offshore winds case is smaller ( $6.25 \text{ m s}^{-1}$ ) than that for the onshore winds ( $9.57 \text{ m s}^{-1}$ ), and the water depth is fairly small, which might suggest relatively low importance of hydrodynamic loads. Possible reasons include (i) the complex wave kinematics at the site because of the shallow water and the steeply sloping sea bed and (ii) wind-wave misalignment. Camp *et al.*<sup>2</sup> showed that the wind and wave directions for the offshore winds at the Blyth site are generally misaligned, in contrast to onshore wind conditions where wind and wave directions are generally aligned, because of the larger fetch associated with onshore winds. Because the wind turbine response variable (a component of the mudline moment) studied here has a fixed orientation in space, the misalignment of the wave load relative to the wind load can act to reduce the net bending moment at the point under consideration. If this occurs, it is then possible that higher waves might lead to lower bending moments,

and vice versa, for offshore wind conditions. This might, in part, also explain why the significant cells (see Figure 4) for offshore winds are associated with low values of significant wave height. In addition to wind–wave misalignment, several other factors specific to the Blyth site might influence turbine loads. One such factor is that the turbine is located in shallow water (about 9 m), on a very sharply sloping sea bed, where changes in the mean water level can lead to significant changes in the wave kinematics and in hydrodynamic loads. It was, in fact, found from the data that the low wave heights causing the larger loads are generally associated with relatively higher mean water levels. Furthermore, this turbine location experiences breaking waves that cause impact loads on the tower. Because of all of these factors, the resulting lateral hydrodynamic loads on the tower are rather complex in nature.<sup>7</sup> If one were to model these various effects, additional random variables (such as the inclusion of wave period, wave spreading/directionality parameters, etc.) that define such more complex environmental conditions would need to be considered. However, data required for these variables, as well as for characteristics such as wind–wave misalignment discussed above, were not available in the summary data from the Blyth site—as such, the effect of these variables on turbine loads could not be systematically studied here.

Finally, the nature and quantity of the recorded data place severe limitations on the analysis based on such data. While the 10 min environmental and turbine load statistics were recorded at the Blyth site for a period of 16 months, the amount of good usable data (for which meaningful measurements for all the relevant channels are available) makes up only about 10% of the overall data. These data are thus limited in the sense that they may not represent all the likely environmental conditions at this site. If more data were available, confidence bounds on estimates of the parameters used for distributions, and on subsequent quantitative results such as on predicted long-term loads, would be improved. Recognizing that there are limitations in making definitive inferences, the presented analyses here suggest that long-term loads for mudline bending moment, obtained using the statistical load extrapolation procedure, are governed by offshore winds.

## Conclusions

We have used a statistical load extrapolation procedure to estimate long-term extreme loads for an offshore wind turbine using limited field data. The mean wind speed at the nacelle and the significant wave height were used to describe the environment, while the mudline bending moment was used to describe the turbine load of interest. Short-term distributions for the turbine load conditional on the environmental variables were modelled using parametric distributions. Parameters for these distributions, as well as for the environmental random variables, were estimated from the available data, which were extremely limited. Long-term loads, associated with return periods of 20 and 50 years, were obtained.

It was observed that the environmental and response characteristics associated with onshore winds (winds blowing from the sea to the shore) and offshore winds (winds blowing from the shore to the sea) are significantly different. The long-term loads were thus calculated separately for these different wind regimes, and it was found that the offshore winds governed the long-term loads even though the average wind speeds are lower for these wind conditions, compared with those for onshore winds. ‘All-direction’ winds were also studied for the sake of comparison. It was found that, for each wind regime, only a small subset of mean wind speed and significant wave height combinations made dominant contributions to the exceedance probability of a given load level. This was mainly because of the relatively large values of the distribution parameters (modal value and measure of dispersion for the Gumbel model used) for the short-term load conditional on the environmental random variables that were found over a small range of wind speeds and wave heights. It was noted that the estimation of these parameters has limitations as the field data available for such estimation are very limited. The variability in the estimation of the parameters for the short-term load distributions was studied using bootstrap techniques, and it was found that the range of predicted long-term loads for a given return period was very large—a clear manifestation of the lack of sufficient data.

In summary, it was concluded that, within the limitations related to the quantity of field data, offshore winds govern the long-term loads for mudline bending moment for the turbine at the Blyth site. It is worth noting

that certain features specific to the study site, such as the complex wave kinematics and hydrodynamics, as well as possible wind–wave misalignment, might help to explain why offshore winds control long-term turbine loads; however, further studies may be needed to quantify some of these effects.

## Acknowledgements

The authors gratefully acknowledge the financial support provided by a CAREER Award (No. CMS-0449128) from the National Science Foundation and by Grant No. 30914 from Sandia National Laboratories. They also thank Garrad Hassan and Partners Ltd. for providing the data recorded at the Blyth site.

## References

1. Efron B, Tibshirani RJ. *An Introduction to Bootstrap*. Chapman and Hall: New York, 1993
2. Camp TR, Morris MJ, van Rooij R, van der Tempel J, zaaijer M, Henderson A, Argyriadis K, Schwartz S, Just H, Grainger W, Pearce D. Design methods for offshore wind turbines at exposed sites. *Final Report of the OWTES Project*, Garrad Hassan and Partners Ltd., Bristol, UK, November 2003.
3. IEC. *IEC 61400-1, Wind Turbines—Part 1: Design Requirements*, 2005.
4. IEC. *IEC 61400-3, Wind Turbines—Part 3: Design Requirements for Offshore Wind Turbines*, TC88 WG3 Committee Draft, 2005.
5. NDV. *Offshore Standard DNV-OS-J101: Design of Offshore Structures*, June 2004.
6. Agarwal P, Manuel L. The influence of the joint wind–wave environment on offshore wind turbine support structure loads. *Journal of Solar Energy Engineering—Transactions of the ASME* 2008; **130** (3): 031010:1–11, August 2008.
7. Henderson AR (ed.). *Design Methods for Offshore Wind Turbines at Exposed Sites—Hydrodynamic Loading on Offshore Wind Turbines*. Delft University of Technology Section Wind Energy: Delft, The Netherlands, 2003.
8. Fitzwater LM, Winterstein SR. Predicting design wind turbine loads from limited data: comparing random process and random peak models. *Proceedings of the 2001 Wind Energy Symposium*, Reno, NV, January, 2001; 355–364.
9. Moriarty PJ, Holley WE, Butterfield SP. Extrapolation of extreme and fatigue loads using probabilistic methods. *National Renewable Energy Laboratory TP-500-34421*, 2004.